DISCRETE AND CONTINUOUS
DYNAMICAL SYSTEMS SERIES B
Volume **24**, Number **1**, January **2019**

doi:10.3934/dcdsb.2018097

pp. **197–209**

NUMERICAL RESULTS ON EXISTENCE AND STABILITY OF STANDING AND TRAVELING WAVES FOR THE FOURTH ORDER BEAM EQUATION

Aslihan Demirkaya

Department of Mathematics
University of Hartford
200 Bloomfield Avenue, West Hartford, CT 06117, USA

Milena Stanislavova

Department of Mathematics
University of Kansas
1460 Jayhawk Boulevard, Lawrence KS 66045–7523, USA

(Communicated by Stephen Pankavich)

Abstract. In this paper, we study numerically the existence and stability of some special solutions of the nonlinear beam equation: $u_{tt} + u_{xxxx} + u - |u|^{p-1}u = 0$ when $p = 3$ and $p = 5$. For the standing wave solutions $u(x,t) = e^{i\omega t}\varphi_\omega(x)$ we numerically illustrate their existence using variational approach. Our numerics illustrate the existence of both ground states and excited states. We also compute numerically the threshold value ω^* which separates stable and unstable ground states. Next, we study the existence and linear stability of periodic traveling wave solutions $u(x,t) = \phi_c(x+ct)$. We present numerical illustration of the theoretically predicted threshold value of the speed c which separates the stable and unstable waves.

1. **Introduction.**

We consider the nonlinear beam equation

$$u_{tt} + \Delta^2 u + u = f(u), \tag{1}$$

which describes the relationship between the beam's deflection and the applied load. This equation, with a particular nonlinearity was considered first in [7] as a model for the suspension bridge. Numerical evidence in the case of exponential nonlinearity suggests that traveling waves are unstable for small speeds c and exhibit soliton like behavior for speeds near the critical value $\sqrt{2}$. The nonlinear fourth-order beam equation has been studied in the last decade both numerically and analytically, see [6], [1], [3], [5]. It is interesting because the solitary waves of other higher-order equations, such as the KdV equation and the generalized Boussinesq equations satisfy a second-order ODE whereas the solitary waves of the beam equation satisfy a fourth-order elliptic equation. There is no maximum principle available for fourth-order PDEs. Thus the ground states may not necessarily be positive, in fact, they may be oscillatory. There is no explicit formula for the solitary waves and this makes

2010 *Mathematics Subject Classification.* Primary: 34K28, 34L16, 34D20, 34L16, 35B35, 35C07.

Key words and phrases. Nonlinear beam equation, standing waves, traveling waves, spectral stability, orbital stability.

Stanislavova supported in part by NSF-DMS # 1516245.

it hard to obtain the spectral information as well. In [6], the existence of ground-state solitary traveling wave solutions of (1) in the form $u(x,t) = \varphi(x+ct)$ was shown for $f(u) = |u|^{p-1}u$ using a constrained minimization technique. Some qualitative conditions on the wave speed c which imply orbital stability and instability of the solitary waves were given as well. In a similar manner, the existence and orbital stability of solitary standing waves is also considered. The analysis there relies more on the variational characterization of the ground states rather than the linearized operator. The authors of [5] showed the existence of traveling wave solutions of (1) for a large class of nonlinearities f and for optimal range of speeds c by adapting the Nehari manifold approach, commonly used for second-order problems, to this fourth order problem.

In the current paper, we present some numerical results for the periodic beam equation:

$$u_{tt} + u_{xxxx} + u = |u|^{p-1}u \tag{2}$$

where $(t,x) \in \mathbf{R}^1 \times [-L,L]$. In the first part, we study the existence and stability of the standing wave solutions $u(x,t) = e^{i\omega t}\varphi_\omega(x)$ in the cases $p = 3$ and $p = 5$ for $\omega \in (-1,1)$. Secondly, we study the existence and linear stability of the traveling wave solutions $u(x,t) = \phi_c(x+ct)$ for $p = 3$ when $c \in (-\sqrt{2},\sqrt{2})$. Our assumption is both φ_ω and ϕ_c are even functions. The choice of power for the nonlinearity is motivated by the importance of odd p's in the PDE models and by our goal to make the numerics as simple as possible and still be able to show the numerical values of the theoretically predicted threshold values for stability ω^* and c^* in a nontrivial model of interest. In fact, it is known (see [6]) that values of $p \geq 9$ produce unstable waves only.

2. **Standing wave solutions.**

In this section, we will present our numerical results for the existence and the orbital stability of the standing wave solutions of (2) in the form:

$$u(x,t) = e^{i\omega t}\varphi_\omega(x) \tag{3}$$

where $\varphi_\omega(x)$ is a real-valued periodic function satisfying the boundary condition: $\varphi_\omega(-L) = \varphi_\omega(L)$. Substituting the anzatz (3) into (2), we get

$$\varphi_\omega'''' + (1-\omega^2)\varphi_\omega - |\varphi_\omega|^{p-1}\varphi_\omega = 0 \tag{4}$$

where $x \in [-L,L]$.

2.1. **The existence of standing wave solutions.**

In the whole line case scenario, the existence of smooth and rapidly decaying solutions to (4) were shown in [6]. If φ_0 is a ground-state solution satisfying (3) with $\omega = 0$, then

$$\varphi_\omega = (1-\omega^2)^{1/(p-1)}\varphi_0((1-\omega^2)^{1/4}x) \tag{5}$$

If the equation is considered in $[-L,L]$ with periodic boundary conditions, the existence of smooth spatially periodic standing waves when $\omega \in (-1,1)$ was shown in [4]. In addition, in this paper the authors prove orbital stability for these waves under certain conditions. Our goal here is to illustrate all of the results in [4] numerically and in particular to compute the threshold value ω^* that separates stability and instability regions. The range of $\omega \in (-1,1)$ here is necessary for the existence of these waves since this guarantees that the functional that is minimized is bounded from below.

2.1.1. *Method.* As in [6] for the whole line case, and in [4] for the periodic case, we use a *constrained minimization technique* in order to show numerically the existence of the standing wave solutions of (2) since we only aim to illustrate the above results and to produce a numerical solution that we can then use for the stability calculations. We consider the following minimization problem:

$$\begin{aligned} \underset{u}{\text{minimize}} \quad & I_\omega(u) = \int_{-L}^{L} (u''(x))^2 + (1-\omega^2)u^2(x)dx \\ \text{subject to} \quad & \int_{-L}^{L} u^{p+1}(x)dx = 1 \end{aligned} \tag{6}$$

If ψ is the solution to (6), then $\varphi_\omega = (I_\omega(\psi))^{\frac{1}{p-1}}\psi$ solves (4). We expand ψ in the Fourier basis, **assuming ψ is even,** to get

$$\psi(x) \simeq \sum_{k=-N}^{N} a_k e^{ikx} = a_0 + \sum_{k=1}^{N} 2a_k \cos kx \tag{7}$$

We use Matlab's built-in interior-point algorithm in order to solve the minimization problem (6). Using the Fourier basis requires us to map $[-L, L]$ to $[-\pi, \pi]$. Thus by change of variables, the minimization problem (6) becomes equivalent to:

$$\begin{aligned} \underset{u}{\text{minimize}} \quad & I_\omega(u) = \int_{-\pi}^{\pi} \left(\frac{\pi}{L}\right)^4 (u''(x))^2 + (1-\omega^2)u^2(x)dx \\ \text{subject to} \quad & \int_{-\pi}^{\pi} u^{p+1}(x)dx = 1 \end{aligned} \tag{8}$$

Remark 1. Note that we work in two cases, $p = 3$ and $p = 5$. When L increases, as expected, N also increases. Because of the nonlinear term, we have to deal with more terms in the case $p = 5$ than in the case $p = 3$.

2.1.2. *Results.* Our numerical results show that the minimization problem (8) has global and local minima. If ψ_1 is the global (local) minimizer of (8) where we have $\psi_1 = \sum_{k=-N}^{N} a_k e^{ikx}$, then $\psi_2 = \sum_{k=-N}^{N} b_k e^{ikx}$ satisfying $a_k = \pm b_k$ is also a global (local) minimizer for (8). Both minimizers, local or global, multiplied by the constant $(I_\omega(\psi))^{\frac{1}{p-1}}$ satisfy the equation (4). In Figure 1, we present two standing wave solutions, one derived from the global minimizer and the other derived from the local minimizer for $p = 3$ case when $\omega = 0.5$ and $L = 20\pi$. The global minimizers are referred to as ground states and the local minimizers are the excited states. The stability of both states is of interest, but we will only discuss the stability of the ground states here. We will compare our numerical results with the theoretical predictions in [4] and [6]. In Figure 2, we present the standing wave solutions derived from the global minimizers of the minimization problem (8) as L and ω varies.

2.2. **Orbital stability of standing wave solutions.** For the whole line case scenario in [6], using Grillakis-Shatah-Strauss type arguments, it was shown that the standing waves (5) are orbitally unstable for $p \geq 9$. The waves are orbitally stable for $p < 9$ for $\sqrt{\frac{2(p-1)}{p+7}} < |\omega| < 1$ and orbitally unstable for $0 \leq |\omega| \leq \sqrt{\frac{2(p-1)}{p+7}}$. For such ω and p, the authors of [4] showed that the standing waves are orbitally stable if $d''(\omega) > 0$ where

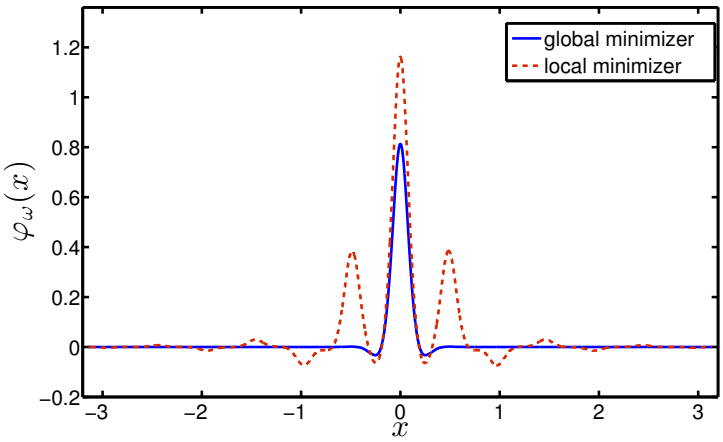

FIGURE 1. Two standing waves are shown for $p = 3$, $\omega = 0.5$ and $L = 20\pi$. The dashed line is the standing wave derived from a local minimizer of (8) and the solid line is derived from a global one.

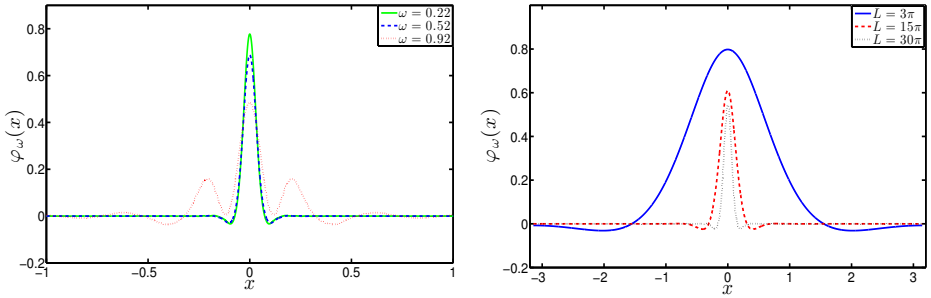

(a) (b)

FIGURE 2. *Existence of standing waves.* φ_ω versus position when $p = 3$, (a) for different values of ω for $L = 50\pi$ (b) for different values of L for $w = 0.8$.

$$d(\omega) = \frac{p-1}{2(p+1)} M(\omega)^{\frac{p+1}{p-1}}, \quad M(\omega) := \inf\{I_\omega(u) : \|u\|_{L^{p+1}} = 1\} \tag{9}$$

for all $p \in (1, +\infty)$ in dimension $d = 1, 2, 3, 4$ and for $1 < p < \frac{2d}{d-4} - 1$, $d \geq 5$ and $\omega \in (-1, 1)$. In Figure 3, one can observe the concavity of $d(\omega)$ for $p = 3$ and $p = 5$ when $L = 50\pi$.

Our numerical computations showed that for any L, there exists ω^* such that if $\omega > \omega^*$ then $d''(\omega) > 0$ and we observed ω^* decreases as L increases. In Table 1, we give some ω^* values for different L values.

Claim. *Based on our numerical results, the relation between ω^* and L is found as*

$$\omega^* = \sqrt{\frac{2(p-1)}{p+7}} \left(1 + \frac{C}{L}\right) \tag{10}$$

where $C = C(L, p)$.

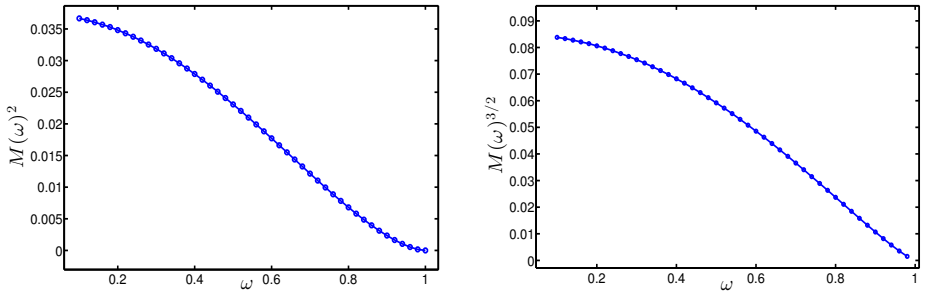

(a) (b)

FIGURE 3. *Orbital stability of standing wave solutions.* $M(\omega)$ versus ω when $L = 50\pi$, (a) $p = 3$, the graph is concave up for $\omega \in (0.64, 1)$, (b) $p = 5$, the graph is concave up for $\omega \in (0.82, 1)$.

p	ω^*	L
3	0.715 ± 0.005	π
	0.655 ± 0.005	$\in [2\pi, 50\pi]$
	0.6375 ± 0.0025	100π
5	0.865 ± 0.005	π
	0.825 ± 0.005	$\in [2\pi, 50\pi]$
	0.8175 ± 0.0025	100π

TABLE 1. ω^* values as L varies.

Remark 2. When $L \to \infty$, ω^* becomes equal to $\sqrt{\frac{2(p-1)}{p+7}}$ which is the case in [6] (see also [4]).

2.3. **Space-time evolution of standing waves.** In order to support our claim for ω^* as in (10), we have checked the space-time evolution of the periodic standing wave solutions for $\omega > \omega^*$ and $\omega < \omega^*$. For our calculations, we mapped the space domain $[-L, L]$ to $[-\pi, \pi]$. We picked $L = 30\pi$ where the claimed ω^* is around 0.66 for $p = 3$ and 0.83 for $p = 5$. Figure (4) (a) shows snap-shots from the simulation of the periodic standing wave moving in time for $\omega = -0.85$, $p = 3$. Figure (4) (b) is the space-time evolution of this standing wave and one can see that the wave is orbitally stable. However when we picked $\omega = 0.55$, we observed that the standing wave is not orbitally stable. Figure (5) (a) presents the corresponding space-time evolution. Similarly we repeated the process for $p = 5$. We picked $\omega = -0.95$ and as shown in Figure 6, we observed that the standing wave is orbitally stable. However, when we picked $\omega = 0.65$, as in Figure 5 (b), we observed that the periodic standing wave is not orbitally stable.

3. **Traveling wave solutions.** In this section, we study the traveling wave solutions $u(x, t) = \phi_c(x + ct)$ of (2) when $p = 3$. These waves satisfy the equation

$$\phi_c'''' + c^2\phi_c'' + \phi_c = \phi_c^3 \tag{11}$$

where $\phi_c(-L) = \phi_c(L)$ and $0 \leq |c| < \sqrt{2}$. As before, the range for wave speed $\in (-\sqrt{2}, \sqrt{2})$ is required so that the functional that is being minimized in the constrained minimization procedure has a bound from below.

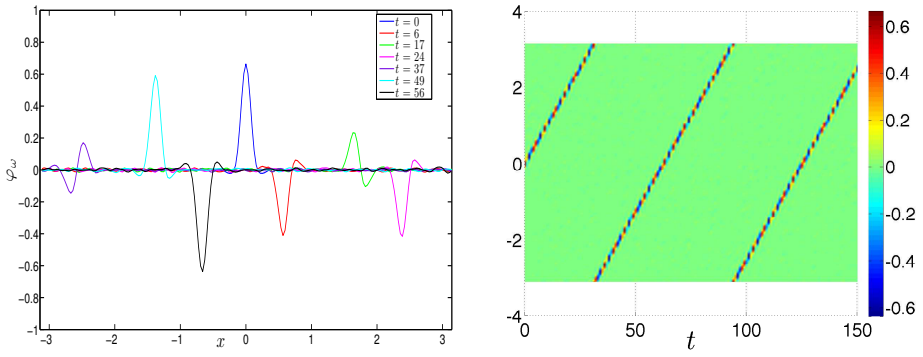

(a) (b)

FIGURE 4. (a) Snap-shots from the simulation of a periodic standing wave for $p = 3$, $\omega = -0.85$, $L = 30\pi$ when $t = 0$ (blue), $t = 5$ (red), $t = 17$ (green), $t = 24$ (pink), $t = 37$ (purple), $t = 49$ (cyan), $t = 56$ (black). (b) the space-time evolution of the periodic standing wave.

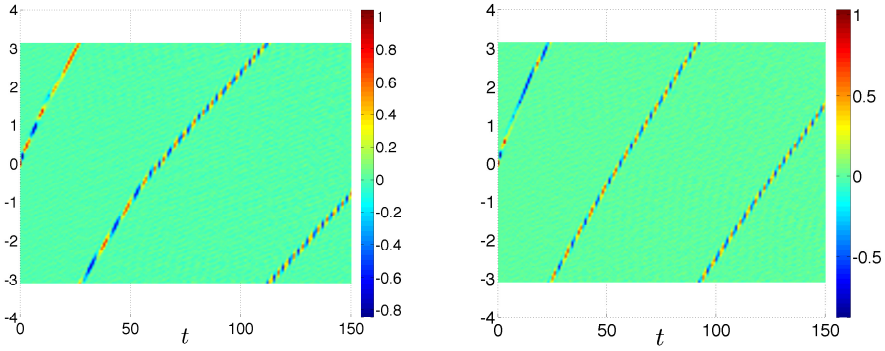

(a) (b)

FIGURE 5. Space-time evolution of the standing wave for $L = 30\pi$ (a) $p = 3$, $\omega = -0.55$ (b) $p = 5$, $\omega = -0.65$

3.1. **Existence of traveling wave solutions.** We need to show the existence of solutions to (11). We will identify (11) as an Euler-Lagrange equation for the following minimization problem

$$\begin{aligned} I_c(u) &= \int_{-L}^{L} (|u''(x)|^2 - c^2|u'(x)|^2 + |u(x)|^2)dx \to \min \\ \textit{subject to } K(u) &= \int_{-L}^{L} |u(x)|^4 dx = 1 \end{aligned}$$

where $c \in (-\sqrt{2}, \sqrt{2})$. We have by Sobolev embedding

$$\|u\|_{L^4([-L,L])} \leq C\|u\|_{H^2[-L,L]}.$$

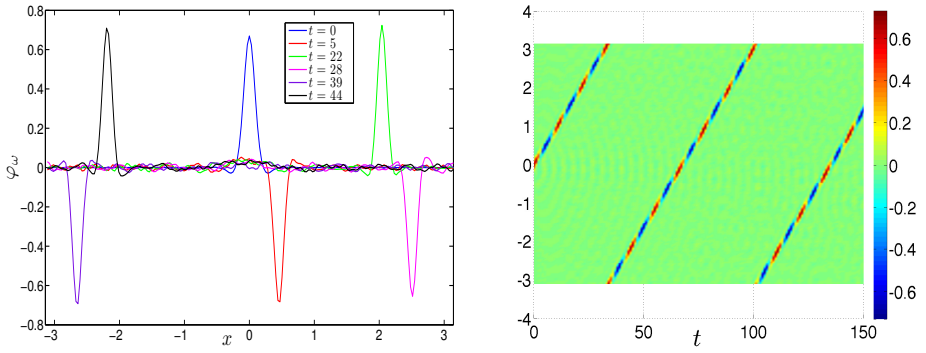

(a) (b)

FIGURE 6. (a) Snap-shots from the simulation of a periodic standing wave for $p = 5$, $\omega = -0.95$, $L = 30\pi$ when $t = 0$ (blue), $t = 5$ (red), $t = 22$ (green), $t = 28$ (pink), $t = 39$ (purple), $t = 44$ (black). (b) the space-time evolution of the periodic standing wave.

Note that $\int_{-L}^{L} u'(x)^2 dx = -\int_{-L}^{L} u(x)u''(x)dx \leq \frac{1}{2}\int_{-L}^{L} u(x)^2 dx + \frac{1}{2}\int_{-L}^{L} u''(x)^2 dx$. Thus one can estimate

$$I_c(u) \geq \int_{-L}^{L} (|u''(x)|^2 - \frac{c^2}{2}|u''(x)|^2 - \frac{c^2}{2}|u(x)|^2 + |u(x)|^2)dx \geq (1 - \frac{c^2}{2})\|u\|_{H^2[-L,L]}.$$

Thus $I_c(u)$ is bounded from below for each admissible u and for $c \in (-\sqrt{2}, \sqrt{2})$. We conclude that the quantity

$$I_c^{\min} := \inf_{\|u\|_{L^4}=1} I_c(u) > 0,$$

is well-defined. Take a smooth minimizing sequence u_n, that is, $\|u_n\|_{L^4} = 1$, and

$$I_c(u_n) \to I_c^{\min}.$$

In particular, we have that $\sup_n \|u_n\|_{H^2} < \infty$. We first take an H^2 weakly convergent subsequence, denoted again by u_n, $u_n \to u$. By the compactness of the embedding $H^2[-L, L] \hookrightarrow L^4[-L, L]$, we can select a convergent (in the topology of $L^4[-L, L]$) subsequence, let us denote it again by u_n, $u_n \to u$. Clearly $u : \|u\|_{L^4} = 1$ and by the lower-semicontinuity of the norms with respect to weak convergence, we have

$$I_c \leq \liminf_n I_c(u_n) = I_c^{\min},$$

whence u is an actual solution of the minimization problem.

The standard Euler-Lagrange scheme then produces a periodic solution of the equation

$$u'''' + c^2 u'' + u = u^3.$$

Setting $\phi_c = \sqrt{I_c^{\min}}u$ gives a solution of (11), for which we have already shown $\phi_c \in H^2[-L, L]$.

3.1.1. *Method.* Similar to the standing waves case, we used the *constrained minimization technique* and worked on:

$$\begin{aligned} \underset{u}{\text{minimize}} \quad & J(\psi) = \int_{-\pi}^{\pi} \left(\frac{\pi}{L}\right)^4 (\psi'')^2 - c^2 \left(\frac{\pi}{L}\right)^2 (\psi')^2 + \psi^2 dx \\ \text{subject to} \quad & \int_{-\pi}^{\pi} \psi^4(x) dx = 1 \end{aligned} \tag{12}$$

to verify the numerical existence of the traveling waves ϕ_c that solve (11) where $\phi_c = \sqrt{J(\psi)}\psi$.

Similar to the standing waves case, we used Fourier basis to expand ψ, assuming that ψ is even. In order to solve the minimization problem (12), as in the standing waves case, we used Matlab's built-in interior-point algorithm.

3.1.2. *Results.* Our numerical results show that the minimization problem (6) has global and local minima and both minimizers, local or global, after multiplied by the constant $\sqrt{J(\psi)}$, satisfy the equation (11). In Figure 7, we see the traveling waves derived from the global minimizers of (12).

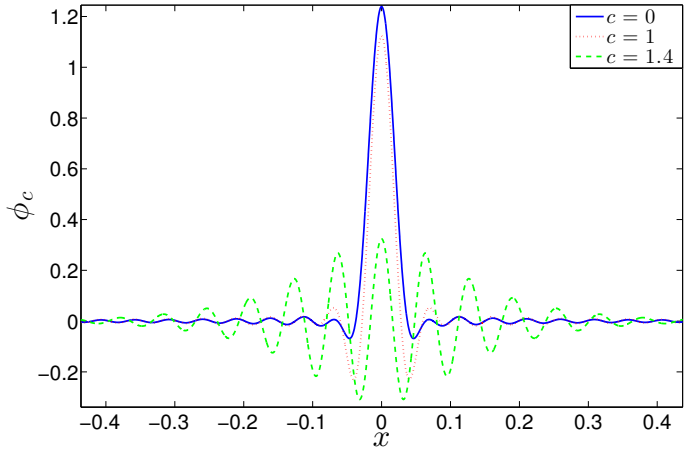

FIGURE 7. *Existence of traveling waves.* ϕ_c versus position for different values of c when $L = 100\pi$ and $p = 3$. $c = 0$ corresponds to the steady state solution.

3.2. **Linear stability of traveling wave solutions.** In order to find the linear stability of the traveling wave solutions ϕ_c, first we study the spectrum of the linearized operator about ϕ_c. If we substitute $u(x,t) = \phi_c(x+ct) + v(x+ct,t)$ into (2) with $p = 3$, we get

$$v_{tt} + 2cv_{tx} + c^2 v_{xx} + v_{xxxx} + v - ((\phi_c + v)^3 - \phi_c^3) = 0 \tag{13}$$

Then the linearized equation becomes:

$$v_{tt} + 2cv_{tx} + \mathcal{H}v = 0 \tag{14}$$

where $\mathcal{H} = D^4 + c^2 D^2 + 1 - 3\phi_c^2$.

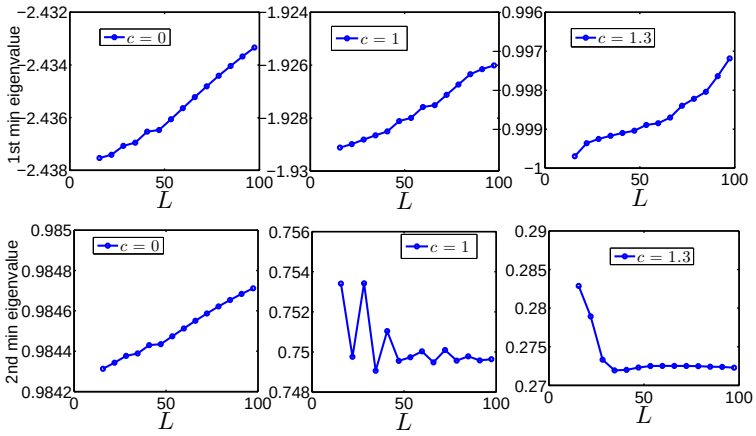

FIGURE 8. The first and the second minimum eigenvalues of $\mathcal{H}$ as L varies on $[5\pi, 31\pi]$ for $c = 0$, $c = 1$ and $c = 1.3$.

3.2.1. *Spectrum of the linear operator $\mathcal{H}$.* Since $\mathcal{H}$ is a fourth order operator, and ϕ' is oscillatory, it is not trivial to obtain its spectrum. For example we cannot apply Sturm-Liouville Theory as we do for the second order operators. Classical results on periodic self-adjoint operators (see for example [8]) provide us with the following.

- There is no essential spectrum since the perturbation has the same period.
- Since $\mathcal{H}$ is a self adjoint operator with domain $D(\mathcal{H}) = H^4_{per}[-L, L]$, an isolated point in the spectrum of $\mathcal{H}$ is also an eigenvalue and it is real.
- 0 is the eigenvalue of $\mathcal{H}$ with the eigenfunction ϕ_c'. Since we assume that ϕ_c is even, we can restrict $\mathcal{H}$ to the even subspace and 0 is not an eigenvalue.
- The bottom of the spectrum of $\mathcal{H}$ is a negative number. Indeed,

$$\langle \mathcal{H}\varphi, \varphi \rangle = -2 \int_{-L}^{L} \varphi^4(x) dx < 0,$$

hence $\sigma(\mathcal{H}) \cap (-\infty, 0) \neq \emptyset$. Unfortunately, we cannot verify analytically that this eigenvalue is simple, although this is easily seen in our numerical simulations, for all values of the parameter c.

3.2.2. *Results.* Our numerical results showed that $\mathcal{H}$ has only one negative eigenvalue for any $c \in (0, \sqrt{2})$ and $L > 0$ and, that eigenvalue is simple. We observed that for any $c \in (0, \sqrt{2})$, there exists a monotonicity between the minimum eigenvalue and the period L and also a monotonicity between the minimum eigenvalue and c. In other words, as c and L increase, the minimum eigenvalue approaches to 0 monotonically. Based on that observation, we became interested in the question: Are there any c and L values such that the minimum eigenvalue is positive? Because of the monotonicity we observed, we focused on c values close to $\sqrt{2}$ and L values arbitrarily large. Numerical calculations show that the minimum eigenvalue of $\mathcal{H}$ when $c = 1.4$ as L varies on $[\pi, 400\pi]$ remained around -0.118. Note that we worked on positive c values, since the operator $\mathcal{H}$ is quadratic in c, so our results are also true for $c \in (-\sqrt{2}, 0)$.

3.2.3. *Stability/Instability results.* In [9], and in more general situations in [10], it is proved that there exists a threshold value of the speed which divides the intervals of stability and the intervals of instability. Following these papers, consider linear, second-order in time equations in the general form

$$u_{tt} + 2\omega u_{tx} + \mathcal{H}u = 0, (t,x) \in \mathbf{R}^1 \times \mathbf{R}^1 \quad \text{or} \quad \mathbf{R}^1 \times [-L, L] \tag{15}$$

where $\mathcal{H} = \mathcal{H}_c$ is a self-adjoint operator acting on L^2, with domain $D(\mathcal{H})$ and ω is a real parameter. Note that it is better at this point to consider ω as an independent parameter, and to ignore the fact that in the applications $\omega = c$.

The self-adjoint operator $\mathcal{H}$ has one simple negative eigenvalue, a simple eigenvalue at zero and the rest of the spectrum is contained in $(0, \infty)$, with a spectral gap. In addition,

$$\begin{cases} \sigma(\mathcal{H}) = \{-\delta^2\} \cup \{0\} \cup \sigma_+(\mathcal{H}), \sigma_+(\mathcal{H}) \subset (\sigma^2, \infty), \sigma > 0 \\ \mathcal{H}\phi = -\delta^2\phi, \ \dim[Ker(\mathcal{H} + \delta^2)] = 1 \\ \mathcal{H}\psi_0 = 0, \ \ \dim[Ker(\mathcal{H})] = 1 \\ \|\phi\| = \|\psi_0\| = 1 \end{cases} \tag{16}$$

We shall need the following spectral projection operators

$$P_0 : L^2 \to \{\phi\}^\perp; P_0 h := h - \langle h, \phi\rangle \, \phi$$
$$P_1 : L^2 \to \{\phi, \psi_0\}^\perp; P_1 h := h - \langle h, \phi\rangle \, \phi - \langle h, \psi_0\rangle \, \psi_0$$

Our next assumption is essentially that $\mathcal{H}$ is of order higher than one. We put it in the following form: for all $\tau >> 1$, we require

$$(\mathcal{H} + \tau)^{-1/2} \partial_x (\mathcal{H} + \tau)^{-1/2}, (\mathcal{H} + \tau)^{-1} \partial_x \in \mathcal{B}(L^2), \tag{17}$$

Note that the quantities in (17) are well-defined, since for all $\tau >> 1$, we have that $\mathcal{H} + \tau \geq (\tau - \delta^2) Id > 0$.

An easy consequence of (17) is that $\mathcal{H}^{-1} P_1 \partial_x P_1 \in \mathcal{B}(L^2)$ as well. This follows easily from the resolvent identity, since

$$\mathcal{H}^{-1} P_1 \partial_x P_1 = P_1 (\mathcal{H} + \tau)^{-1} \partial_x P_1 + \tau \mathcal{H}^{-1} P_1 (\mathcal{H} + \tau)^{-1} \partial_x P_1.$$

Lastly, we assume that H has real coefficients. We formulate as follows

$$\overline{\mathcal{H}h} = \mathcal{H}\bar{h}. \tag{18}$$

An important observation, that we would like to make right away (and which will be used repeatedly in our arguments later on) is that for every $\lambda > 0$, the operator $(\mathcal{H} + \lambda^2) : \{\phi\}^\perp \to \{\phi\}^\perp$ is invertible, since $(\mathcal{H} + \lambda^2)|_{\{\phi\}^\perp} \geq \lambda^2 Id$.

Then we have the following Theorem.

Theorem 3.1. *Let $\mathcal{H}$ be a self-adjoint operator on L^2. Assume that it satisfies the structural assumption (16), (17) as well as (18).*

Then, if[1] *that $\left\langle \mathcal{H}^{-1}[\psi_0'], \psi_0' \right\rangle \geq 0$ we have spectral instability for all values of $\omega \in \mathbf{R}^1$.*

Otherwise, supposing $\left\langle \mathcal{H}^{-1}[\psi_0'], \psi_0' \right\rangle < 0$, we have

- *the problem (15) is unstable if ω satisfies the inequality*

$$0 \leq |\omega| < \frac{1}{2\sqrt{-\left\langle \mathcal{H}^{-1}[\psi_0'], \psi_0' \right\rangle}} =: \omega^*(\mathcal{H}) \tag{19}$$

[1]Note that $\psi_0' \perp \psi_0$ and hence, since $Ker(\mathcal{H}) = span\{\psi_0\}$, $\mathcal{H}^{-1}[\psi_0']$ is well-defined

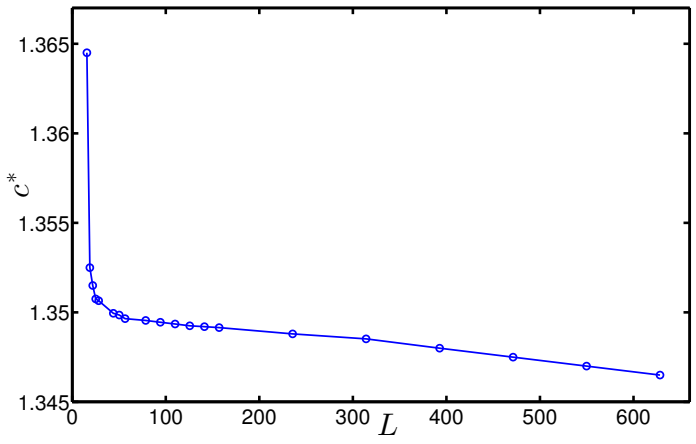

FIGURE 9. c^* *versus* L. In this figure, L varies on $[5\pi, 200\pi]$. The numerical computations show us as L increases c^* decreases.

- *the problem* (15) *is stable, if* ω *satisfies the reverse inequality*

$$|\omega| \geq \omega^*(\mathcal{H}) \tag{20}$$

For the traveling wave solutions of the beam equation considered here, we get the following result.

Theorem 3.2. *Assume that there exists a one parameter family* $\{\varphi_c\}_{c\in I}$ *such that*

- $\varphi_c \in H^1$ *and* $c \to \|\varphi_c'\|_{L^2}$ *is a differentiable function on* I.
- *The operator* $\mathcal{H}_c = \partial_x^4 + c^2\partial_x^2 + 1 - p\varphi_c^{p-1}$ *satisfies* (16).

Then, the wave φ_c *is linearly stable if and only if*

$$\partial_c\|\varphi_c'\| < 0 \quad \textit{and} \quad |c| \geq \frac{\|\varphi_c'\|}{-2\partial_c\|\varphi_c'\|}. \tag{21}$$

That is, if $\partial_c\|\varphi_c'\| \geq 0$ *or* $\partial_c\|\varphi_c'\| < 0$, *but* $|c| < \frac{\|\varphi_c'\|}{-2\partial_c\|\varphi_c'\|}$, *the wave* φ_c *is unstable.*

We should note that the conclusions of our result for the case of the real line coincide with those of Levandosky, [6]. Indeed, he computes $d'(c) = -c\|\varphi_c'\|^2$, whence $d''(c) = -\|\varphi_c'\|(\|\varphi_c'\| + 2c\partial_c\|\varphi_c'\|)$. Clearly, our linear stability conditions are precisely equivalent to $d''(c) > 0$, which by Levandosky's work implies orbital stability.

Since there are no explicit formulas for the traveling wave solutions, the condition (21) is impossible to verify analytically. Instead, we will use the form of the solutions computed above and verify numerically that such threshold speed c^* exists. We already verified numerically that the spectral conditions are satisfied (see fig.8). Next, we worked numerically and showed that there exists c^* such that (21) holds for any $|c| \in [c^*, \sqrt{2}]$. We observed that c^* decreases as L increases. This means as L gets larger, the interval for the stability gets larger. In Figure 9, we show such c^* values as L varies. Note that in [6] it is proved that the waves are unstable for values of c close to zero and stable for values of c close to $\sqrt{2}$. Here we explicitly compute the threshold value $c^* \sim 1.348$ (predicted in [9] and [10]) that separates the unstable from the stable waves.

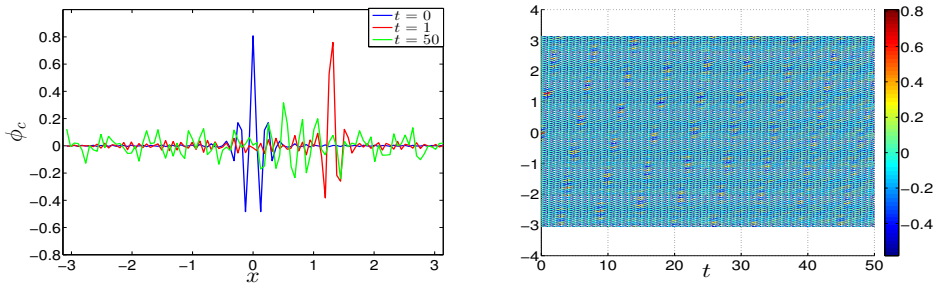

(a) (b)

FIGURE 10. (a) Snap-shots from the simulation of a periodic traveling wave for $c = -1,32$, $L = 30\pi$ when $t = 0$ (blue), $t = 1$ (red) and $t = 50$ (green) (b) the space-time evolution of the periodic traveling wave.

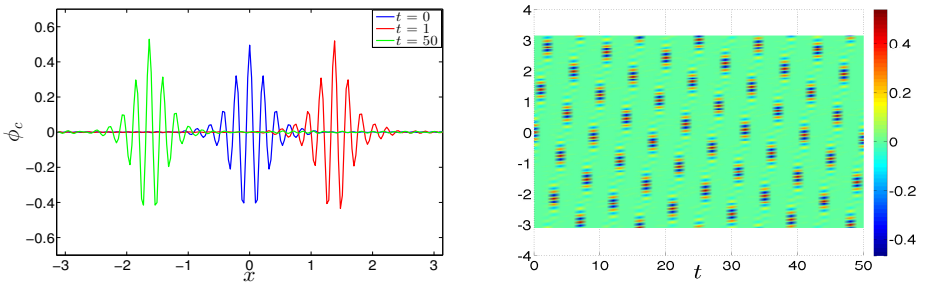

(a) (b)

FIGURE 11. (a) Snap-shots from the simulation of a periodic traveling wave for $c = -1,38$, $L = 30\pi$ when $t = 0$ (blue), $t = 1$ (red) and $t = 50$ (green) (b) the space-time evolution of the periodic traveling wave.

3.3. **Space-time evolution of traveling waves.** As we did for the periodic standing wave solutions, we have been curious about the space-time evolution of the periodic traveling wave solutions for the values less and more than the critical value c^*. We picked $L = 30\pi$ where the claimed c^* is around 1.35. We first ran the simulation for $c = -1.32$. We observed that the traveling wave did not preserve its shape in time as shown in Figure 10. However when we picked $c = -1.38$, (Figure 11) the simulations showed that the periodic wave kept its shape as it traveled in time. The space-time evolution plot also shows that it preserves its shape as it travels in the long time.

REFERENCES

[1] A. R. Champneys, P. J. McKenna and P. A. Zegeling, Solitary waves in nonlinear beam equations: stability, fission and fusion, *Nonlinear Dynam*, **21** (2000), 31–53.

[2] L. Chen, Orbital stability of solitary waves for the Klein-Gordon-Zakharov equations, *Acta Math. Appl. Sinica*, **15** (1999), 54–64.
[3] Y. Chen and P. J. McKenna, Traveling waves in a nonlinearly suspended beam: Theoretical results and numerical observations, *J. Differential Equations*, **136** (1997), 325–355.
[4] S. Hakkaev, M. Stanislavova and A. Stefanov, Orbital Stability for periodic standing waves of the Klein-Gordon-Zakharov and the Beam equation, *ZAMP-Zeitschrift fuer Angewandte Mathematik und Physik,*, **64** (2013), 265–282.
[5] P. Karageorgis and P. J. McKenna, The existence of ground states for fourth-order wave equations, *Nonlinear Anal*, **73** (2010), 367–373.
[6] S. Levandosky, Stability and instability of fourth order solitary waves, *J. Dynamics and Differential Equations*, **10** (1998), 151–188.
[7] P. J. McKenna and W. Walter, Traveling waves in a suspension bridge, *SIAM J. Appl. Math.*, **50** (1990), 703–715.
[8] J. Smoller, *Nonlinear Ordinary Differential Equations*, CRC Press, Boca Raton, FL, 1993.
[9] M. Stanislavova and A. Stefanov, Linear stability analysis for traveling waves of second order in time PDE's, *Nonlinearity*, **25** (2012), 2625–2654.
[10] M. Stanislavova and A. Stefanov, Spectral stability analysis for special solutions of second order in time PDE's: the higher dimensional case, *Physica D: Nonlinear Phenomena*, **262** (2013), 1–13.

Received January 2017; revised July 2017.

E-mail address: demirkaya@hartford.edu
E-mail address: stanis@math.ku.edu